Qualitative photoelastic study of the force system produced by retraction T-springs with different preactivations

Luiz Guilherme Martins Maia*, Vanderlei Luiz Gomes**, Ary dos Santos-Pinto***, Itamar Lopes Júnior****, Luiz Gonzaga Gandini Jr.*****

Abstract

Objective: Evaluate the force system produced by the T-spring used for space closure. **Methods:** By means of the experimental photoelastic method, we evaluated the T-spring—used for space closure—with two different preactivations on its apical portion, i.e., one with 30° and one with 45°. The springs were fabricated with rectangular 0.017 X 0.025-in titanium-molybdenum alloy (TMA), centered in a 27.0 mm interbracket space and activated at 5.0 mm, at 2.5 mm, and in a neutral position. For more reliable results, tests were repeated on three photoelastic models duplicated and prepared by the same operator. To better understand the results, the fringes seen in the polariscope were photographed and analyzed qualitatively. **Results:** Through qualitative analysis of the fringes order in the photoelastic model it was noted that at the retraction and anchoring ends the T-spring with 30° apical activation showed a slightly greater accumulation of energy relative to the force system that was generated.

Keywords: Closing of orthodontic space. T loop. Photoelastic study. Retraction.

INTRODUCTION

The extraction philosophy advocated by Tweed in the 1940s raised a new perspective for orthodontic treatment, arousing the interest of orthodontists in mechanical retraction. Since then several mechanical devices have been developed for this purpose and knowledge about the force system generated by each of them has become a constant focus of research.[16,17]

In performing retraction movements, orthodontists must be knowledgeable of the mechanical principles involved in this system

to ensure that tooth movement occurs with maximum effectiveness and minimum strain on adjacent periodontal tissues.[1,12] Ideally, space closure should be accomplished by retraction movement resulting from "loop" type orthodontic appliances. In this case, forces become predictable as they are in close relationship with archwire size, loop design, alloy type, spring position, amount of activation, force constancy, force magnitude and momentum magnitude.[2,3,10,11,13,14,18-21,23,24]

In "sliding" type retraction appliances, however, the force system that is generated becomes less predictable since the magnitude of force is difficult to measure as part of it is dissipated by friction during movement.[1,12]

Burstone,[2] in 1982, cited three properties that any device should display during retraction movement: a momentum/force ratio, achieved by incorporating Gable-like bends and preactivation bends; force magnitude during activation and a load/deflection ratio, represented by the amount of energy lost during deactivations.

Another important property of the treatment plan is the anchorage type one wishes to obtain to ensure adequate dental relationship.[2,14] In this context, the T-spring designed by Burstone and Koenig[3] adds several ideal efficiency features that optimize space closure. The biomechanical properties of this spring have been the subject of many studies in the orthodontic community and its force system has been widely disseminated[2,3,10,11,19-22,24] in investigations involving mechanical tests[3,10,11,17-24] and finite elements method.[13] Hence the interest in evaluating this system by the experimental photoelastic method.[5-9,15,25]

The T-spring is often utilized in research undertaken at the Graduate Orthodontic Clinic of the School of Dentistry of Araraquara, São Paulo State, Brazil. The purpose of this study was to evaluate, by means of photoelasticity[5-9,15,25], the force system of a T-spring centered in the interbracket space using two different preactivation types.[14,20,21]

MATERIAL AND METHODS

Initially, tests were performed on 5 experimental pilot models in order to determine proper methodology research, materials to be used, number of repetitions needed, model fabrication technique, reading technique and researcher calibration to ensure result accuracy.[15]

Two photoelastic models were obtained from a master model, built of Formica, with the following dimensions: 60.0 mm in length, 40.0 mm in height and 20.0 mm in thickness (Fig 1).

After obtaining a matrix box, we used two acrylic teeth (MOM™, Brazil) to be positioned and bonded to it. With the purpose of standardizing the positioning of these teeth, a negative model was made from the pilot model using ASB-10 Blue silicone rubber and rubber catalyst (POLIPOX™, Brazil) (Fig 2), mixed and manipulated according to manufacturer's recommendations.

In the following step, a utility wax box was made with the following dimensions: 120.0 mm wide, 140.0 mm long and 90.0 mm in height so as to allow the master model to be positioned and the addition silicone subsequently added according to manufacturer's specifications, thereby obtaining the negative model (Fig 3).

At this stage, other teeth were positioned in their respective sites while carefully preventing contamination by moisture or grease on the root surfaces and silicone. At this time, the photoelastic resin (POLIPOX™, Flexible CMR-201, component A code: 584-4. Lot: 17680) and the hardener component (CME-252 Flexible, Code: 1322-6, Lot: 17873) were manipulated in a glass container graduated in milliliters (Fig 4).

Both components were added and carefully manipulated for 10 minutes, and then this mixture was poured into the obtained mold. This mold was placed in an oven at a constant temperature of 25° C for 24 hours for complete curing (Fig 5). In these two phases, the resin was handled carefully to avoid incorporation of air bubbles.

The model was then removed from the mold

FIGURE 1 - Matrix made of Formica to serve as a replicator. Positioning of the canine crowns that will serve as parameters for the photoelastic model.
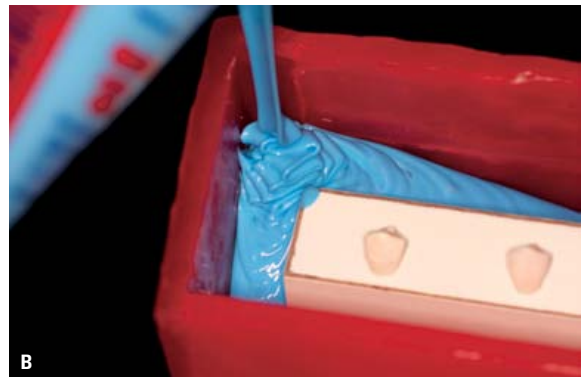

FIGURE 2 - Silicone rubber and catalyst.

FIGURE 3 - Matrix was positioned inside the wax box (**A**) and the silicone (**B**) was poured to obtain a negative.

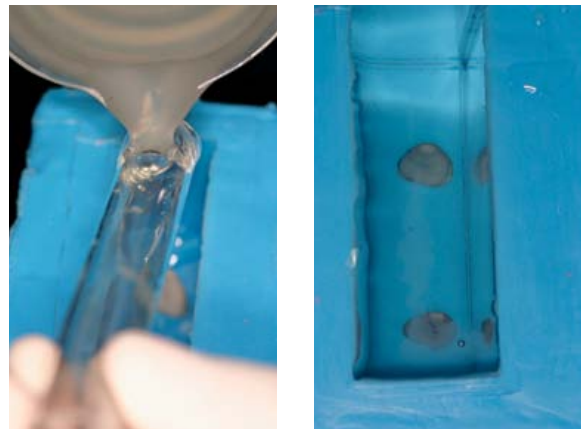FIGURE 4 - Epoxy resin, components A and B.

FIGURE 5 - After epoxy resin manipulation, it was poured carefully to avoid incorporation of air bubbles.

and, at this stage, the optical conditions of the photoelastic model was checked in the polariscope. Should the model fail to produce adequate optical properties,[15] which would undermine the analysis, it would be discarded and the aforementioned steps repeated until an ideal model was produced (Fig 6).

Once both photoelastic models had been defined a Morelli™ (Brazil) 'crossed' tube was attached to each tooth (Fig 7), and to this end, a vertical slot was made using a cylindrical drill at low speed, where the tubes were fitted and bonded with acrylic resin.

For each model, a T-spring made with 0.017 X 0.025-in titanium-molybdenum archwire (TMA)

FIGURE 6 - Photoelastic model.

(Ormco™, Glendora, CA, USA) was used. In order to maintain the standard, the T-springs were made with the aid of a template with the following dimensions: 10.0 mm long and 7.0 mm in height.

Two activation criteria were utilized, i.e., a T-spring with 45 degrees[14,21] preactivation on the apical base was inserted into one model and a T-spring with 30 degrees[20] preactivation on the apical base into the other model (Fig 8).

After checking the T-springs in the neutral position, they were inserted into the horizontal slots of the 'crossed' tubes, centered at an interbracket distance of 27.0 mm[10] and evaluated at three activations: 5.0 mm, 2.5 mm and in neutral position. To ascertain reliability, these tests were repeated twice again and showed identical results.

The tests were performed in the laboratory of Mechanical Engineering, Federal University of Uberlândia-MG (Department of Physics), assessed with a polariscope refraction equipment and photographed with digital Canon Rebel EOS 300D (6.3 mega-pixels, 100.0 mm Canon macro lens and ultrasonic circular Canon Flash Macro Ring Lite MR-14EX) (Fig 9).

RESULTS

The results were obtained by reading the photoelastic fringes in the models using Burstone's[2]
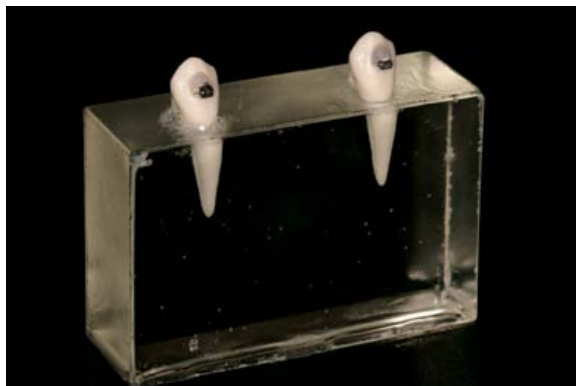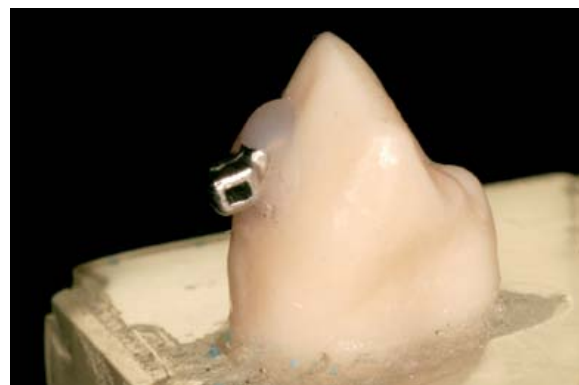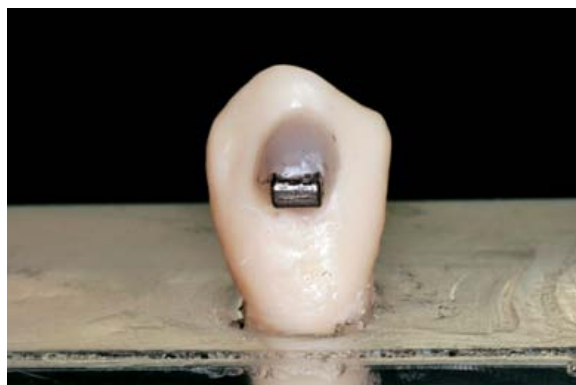

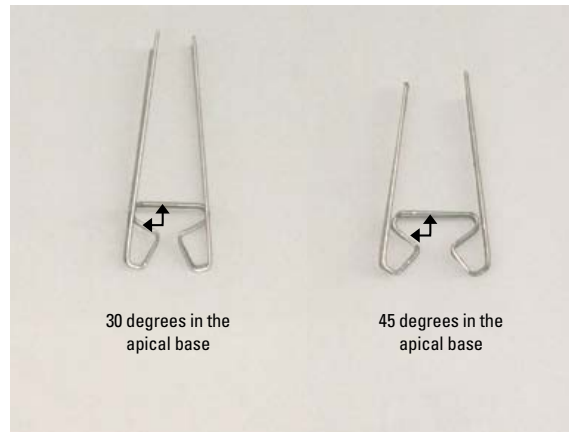FIGURE 7 - Photoelastic model with 'crossed' tubes in position.

FIGURE 8 - Template to standardize the fabrication of Souza standard (30 degrees) and Marcotte standard (45 degrees) T-springs.
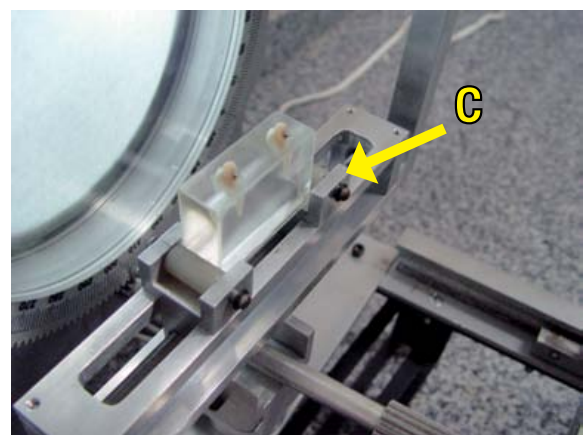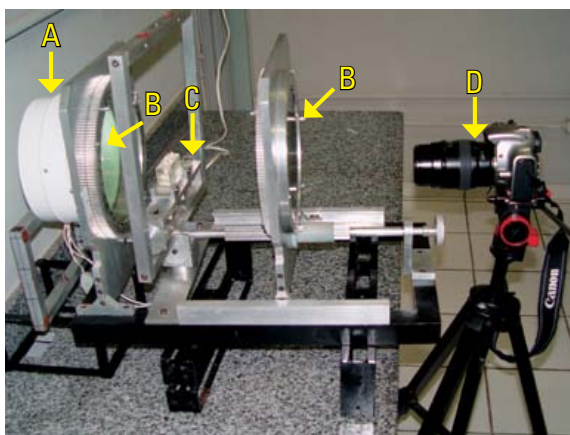

FIGURE 9 - Flat circular polariscope: (**A**) light source, (**B**) polarizers, (**C**) photoelastic model and (**D**) digital photographic equipment.

T-springs with two different types of preactivation.[14,20,21] The spring was analyzed in three different positions: (1) in a neutral position, (2) with 2.5 mm activation, and (3) with 5.0 mm activation.

The interpretations were evaluated descriptively and the readings made in charts divided into the three portions of each tooth, i.e., one mesial, one apical and one distal, which were evaluated one by one separately and then compared with the adjacent teeth (Fig 10).

The reading of the fringes order was accomplished through the interface of the violet and blue colors, formed on the distal, mesial and apical surfaces of each tooth, using the distance as reference for building the analysis charts. On an increasing scale, the following colors are formed: black, yellow, red, blue, yellow, red, green, yellow, red and green (Fig 11).

Figure 12 shows the fringe order of 0.0 in the photoelastic model due to the absence of a T-spring. In this case, the photoelastic model is free from any force interference.

Figure 13 represents a photoelastic model free

of tension, where the fringe order is 0.0 across the root surface of both teeth.

Fringe order and interpretation of the T-spring with preactivation recommended by Souza et al[20]

In neutral position, the T-spring, with the preactivation proposed by Souza et al[20] exhibited a fringe order of 0.5 across the full root surface. This means that in this qualitative analysis, although stress was equally distributed from the cervical region down to the root apex, it suggests to us that a small amount of energy or a very low force

magnitude was applied to these teeth (Fig 15).

The representation in Figure 14 shows that the T-spring with preactivation recommended by Souza et al,[20] in the neutral position, formed a fringe order of 0.0 across the mesial surface, except the cervical mesial region of tooth 23. In this region, the fringe order ranged from 0.0 to 0.5 and had no relevance.

Figure 16 shows that the T-spring with Souza et al's[20] preactivation in a neutral position generated a fringe order of 0.0 across the full apical extension for both teeth.

Figure 18 demonstrates that the T-spring with Souza et al's[20] preactivation in a neutral position presented a fringe order of 0.0 across the full distal extension.

Analyzing Figure 17, it can be observed that in the cervical and middle thirds of teeth 13 and 23 the fringe order ranges from 1.5 to 2.0. On the other hand, in the distal apical region of teeth 13 and 23 the fringe order is 0.5, which reflects a reduced amount of energy generated in that region suggesting a controlled tipping movement. A slight asymmetry was observed in the distal apical region of tooth 13 but with no significance to the qualitative analysis. It is suggestive of asymmetric activation or slightly decentered positioning, or perhaps some interference while fabricating the spring.
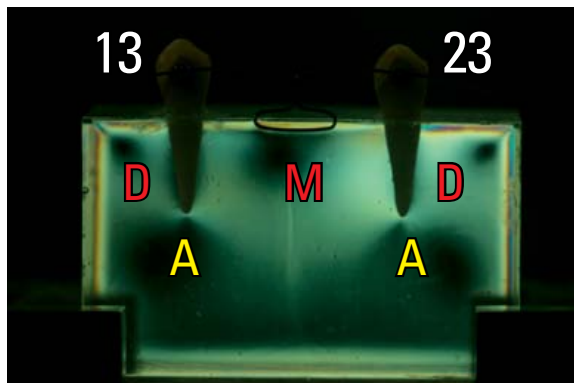

FIGURE 10 - Nomenclature suggested for reading and interpreting fringe order on the photoelastic model.
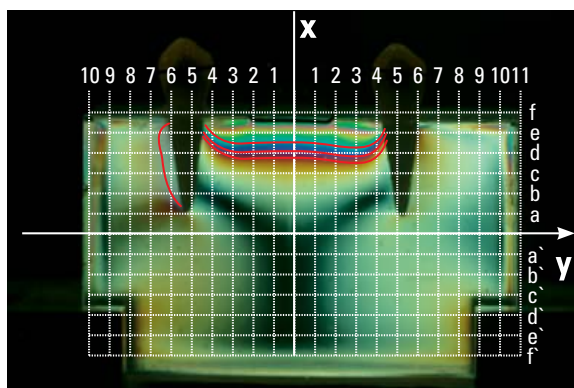

FIGURE 11 - Layout of the Cartesian axis to facilitate the reading of fringe order points on the photoelastic model.
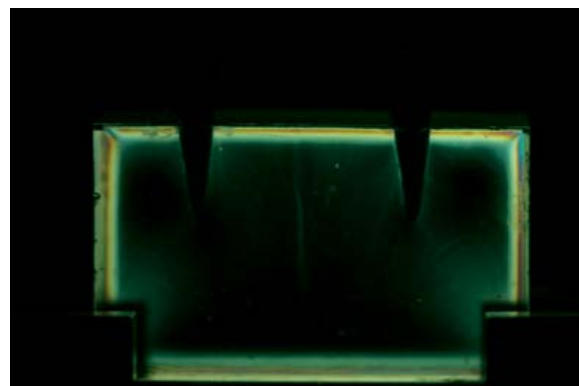

FIGURE 12 - Fringe order of 0.0 due to the absence of a T-spring, as observed through the polariscope.
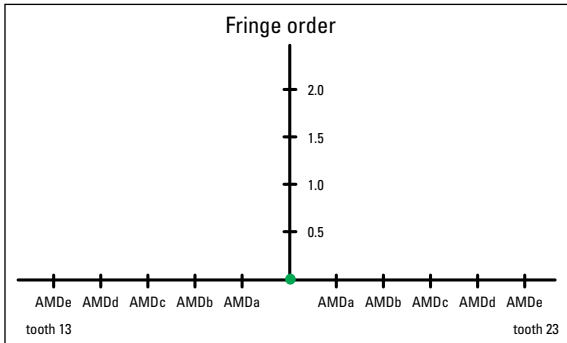
FIGURE 13 - The green point in the vertex of the chart represents fringe order equal to zero.
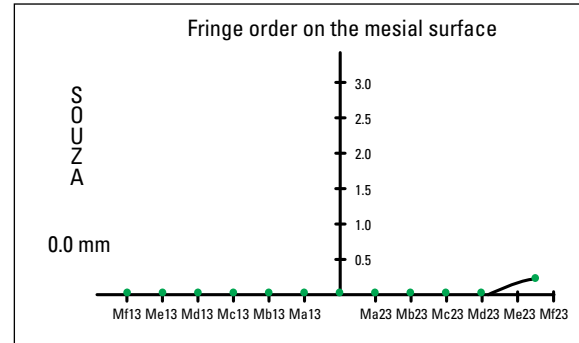

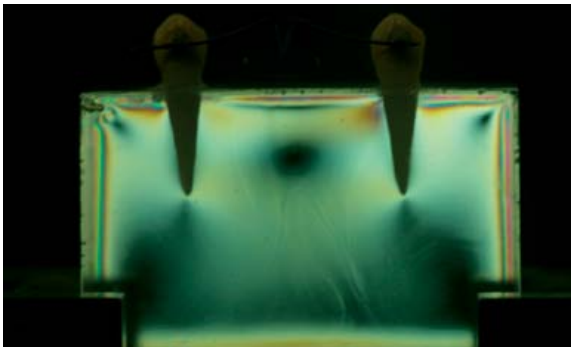FIGURE 14 - Representation of the mesial surface with Souza's preactivation in neutral position.

FIGURE 15 - Activation in neutral position (0.0 mm activation).
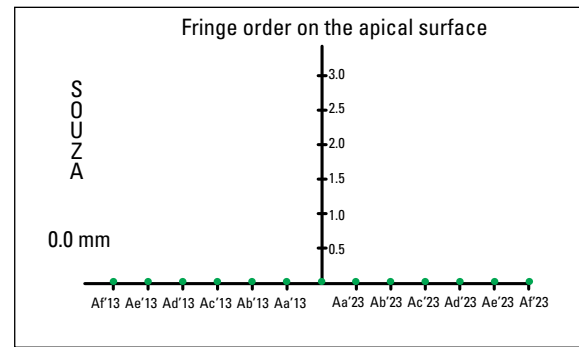

FIGURE 16 - Representation of the apical surface with Souza's preactivation in neutral position.

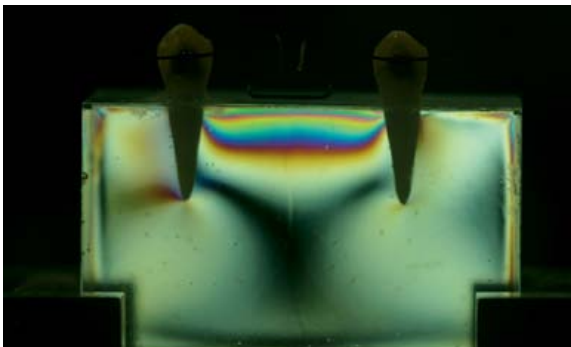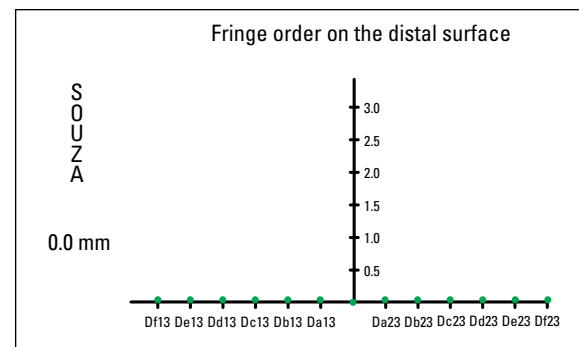FIGURE 17 - T-spring activation at 2.5 mm.

FIGURE 18 - Representation of the distal surface with Souza's preactivation in neutral position.
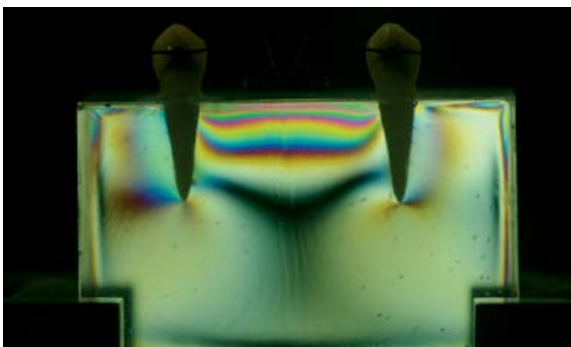

FIGURE 19 - T-spring activation at 5.0 mm (maximum activation).

Figure 20 describes a T-spring with 2.5 mm activation and preactivation proposed by Souza et al[20] showing a concentration of fringes at 1.5, with the fringe order spread out in a symmetrical pattern.

Figure 21 depicts a T-spring with activation of 2.5 mm and with pre-activation proposed by Souza et al[20] forming a fringe concentration close to 0.0, but discretely greater for tooth 13.

In Figure 22 a T-spring is shown with 2.5 mm activation and preactivation proposed by Souza et al[20] presenting a concentration of fringes at 0.5 on the distal cervical third of tooth 23, along with a fringe order of 0.5 on the distal lower third of tooth 13.

Figure 19 shows a fringe order slightly greater than 2.5, demonstrating that a T-spring with 30º preactivation displays a greater accumulation of energy than one with 45º preactivation, in the same activation.

In Figure 23 a T-spring with 5.0 mm activation and preactivation proposed by Souza et al[20] showed a concentration of fringes ranging from 0.5 on the middle third root region to 2.5 on the cervical middle third region.

Figure 24 shows a T-spring with 5.0 mm activation and preactivation proposed by Souza et al[20] demonstrating a concentration of fringes ranging from 0.0 to 0.5 for tooth 23 and slightly greater than 0.5 on the apical region, for tooth 13.

Figure 25 depicts a T-spring with 5.0 mm activation and preactivation proposed by Souza et al[20] showing a concentration of fringes at 0.5 across the full extension of the distal root surface of teeth 23 and 13.

Fringe order and interpretation of the T-spring with preactivation recommended by Marcotte[14]

In neutral position, the T-spring with the pre-activation proposed by Marcotte[14] exhibited a fringe order of less than 0.5 across the full root surface. This means that in this qualitative analysis, although stress was equally distributed from the cervical region down to the root apex, it suggests to us that a small amount of energy or a very low force magnitude was applied to these teeth (Fig 29).

FIGURE 20 - Representation of the mesial surface with Souza's preactivation and 2.5 mm activation.

FIGURE 21 - Representation of the apical surface with Souza's preactivation and 2.5 mm activation.

FIGURE 22 - Representation of the distal surface with Souza's preactivation and 2.5 mm activation.

Figure 26 is a representation of T-spring with Marcotte's[14] preactivation in neutral position, exhibiting across the full mesial extension a fringe order of 0.0.

In Figure 27 a representation of T-spring with Marcotte's[14] preactivation in neutral posi-
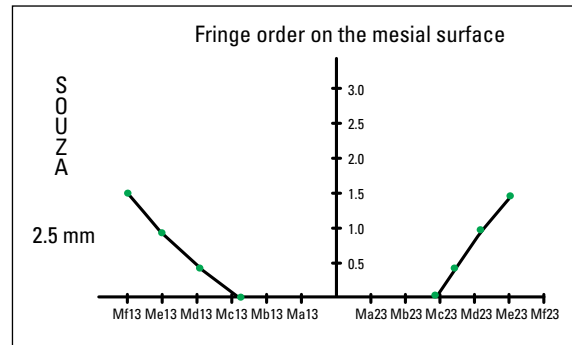
Fringe order on the mesial surface

FIGURE 23 - Representation of the mesial surface with Souza's preactivation and 5.0 mm activation.

Fringe order on the mesial surface

FIGURE 26 - Representation of the mesial surface with Marcotte's preactivation in neutral position

Fringe order on the apical surface

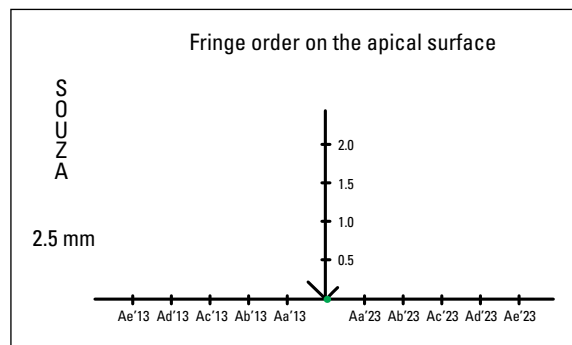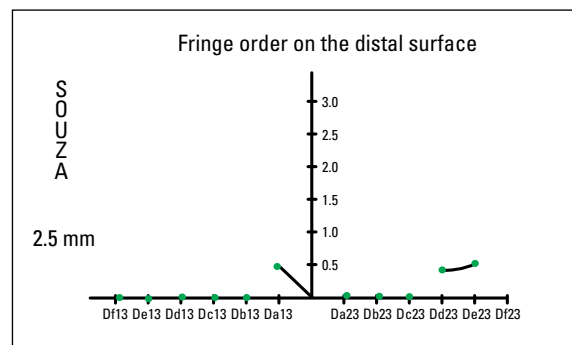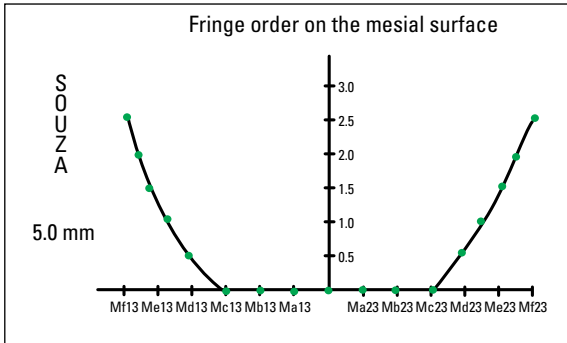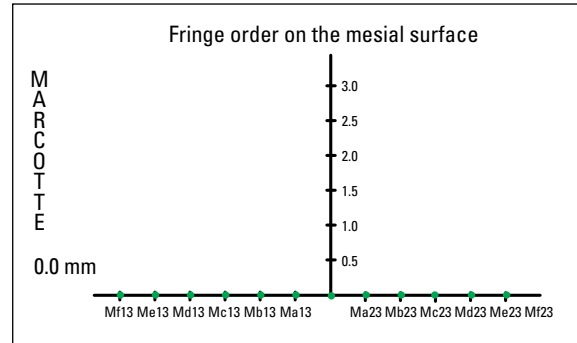FIGURE 24 - Representation of the apical surface with Souza's preactivation and 5.0 mm activation.

Fringe order on the apical surface

FIGURE 27 - Representation of the apical surface with Marcotte's preactivation in neutral position.

Fringe order on the distal surface

FIGURE 25 - Representation of the distal surface with Souza's preactivation and 5.0 mm activation.

Fringe order on the distal surface
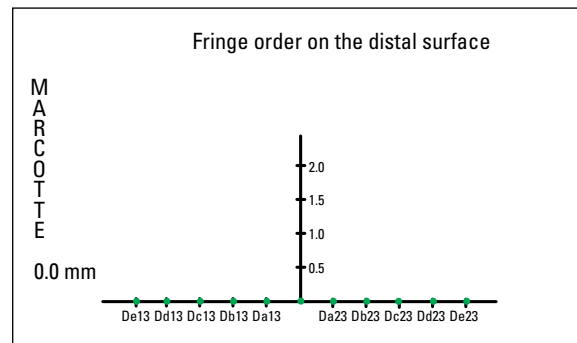
FIGURE 28 - Representation of the distal surface with Marcotte's preactivation in neutral position.

tion, exhibiting across the full apical extension a fringe order of 0.0.

Figure 28 is the graphical representation of T-spring with Marcotte's[14] preactivation in neutral position, exhibiting across the full distal extension a fringe order of 0.0.

Figure 30 shows a fringe order slightly smaller than 1.5, demonstrating that a T-spring with 45° preactivation displays a slightly smaller energy accumulation than one with 30° preactivation, when activated at 2.5 mm.

Figure 32 demonstrates a T-spring activated
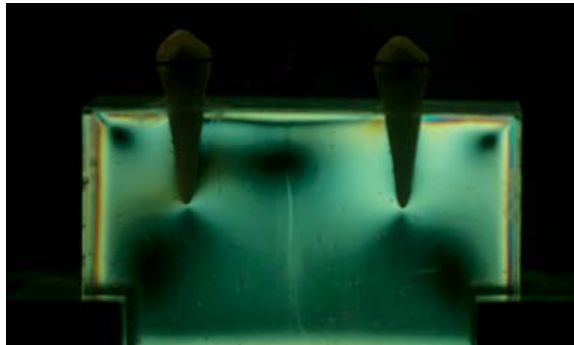
FIGURE 29 - Activation in neutral position (0.0 mm activation).
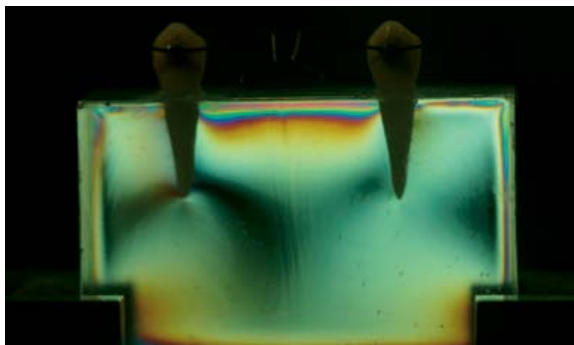
FIGURE 30 - T-spring activation at 2.5 mm.
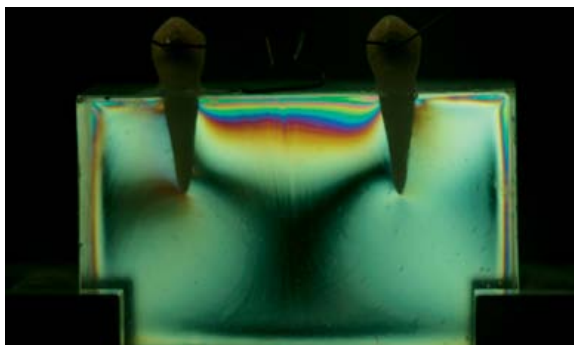
FIGURE 31 - T-spring activation at 5.0 mm.

2.5 mm according to Marcotte[14] showing a fringe concentration ranging from 0.0 in the middle third of the root surface to 1.5 in the cervical third.

Figure 33 shows a T-spring with 2.5 mm activation and pre-activation proposed by Marcotte[14]

generating a concentration of fringes close to 0.0 on the apical third.

In Figure 34 it can be seen that a T-spring with Marcotte's[14] preactivation at 2.5 mm presented a fringe order of 0.0 along the full distal extension.

Figure 31 shows a fringe order smaller than 1.5, demonstrating that a T-spring with 45° preactivation displays a slightly decreased accumulation of energy than one with 30° preactivation, when activated at 2.5 mm. When comparing Figures 30 and 31 a different fringe order between 2.5 mm and 5.0 mm activation was observed when using Marcotte's[14] recommended preactivation. The 5.0 mm activation involved a greater amount of energy.

In Figure 35, a T-spring with 5.0 mm activation and preactivation advocated by Marcotte[14] can be observed. It shows a concentration of fringes ranging from 0.0 on the middle third to 1.5 on the cervical third. A comparison between this figure and Figure 23 shows that the fringe order was more intense for T-springs preactivated according to Souza et al,[20] activated at 5.0 mm, revealing that these springs generate a greater amount of energy.

Figure 36 represents a T-spring with 5.0 mm activation and preactivation advocated by Marcotte.[14], revealing a concentration of fringes ranging from 0.0 to 0.5 on the apical third, although more energy was observed in tooth 13.

Figure 37 shows a T-spring with 5.0 mm activation and preactivation proposed by Marcotte[14], revealing a concentration of fringes of nearly 0.5 on the distal cervical third of tooth 23, and a fringe order of 0.5 on the distal surface of the lower third of tooth 13.

By analyzing each figure, it was noted that for both pre-activations the energy concentration that is delivered is very similar and occurs symmetrically in all tests. The presence of a slight asymmetry was observed, possibly due to a slight decentralization of the spring upon installation and/or activation, or perhaps such asymmetry occurred during the spring fabrication process.
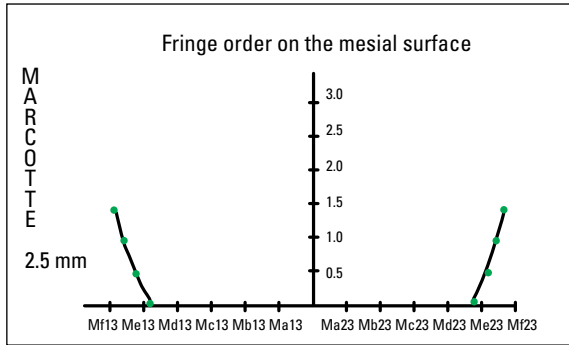
FIGURE 32 - Representation of the mesial surface with Marcotte's preactivation and 2.5 mm activation.
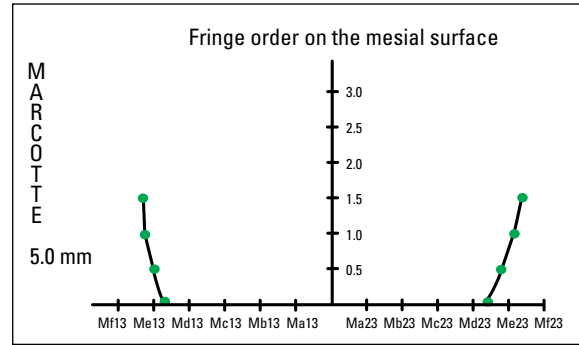
FIGURE 35 - Representation of the mesial surface with Marcotte's preactivation and 5.0 mm activation.
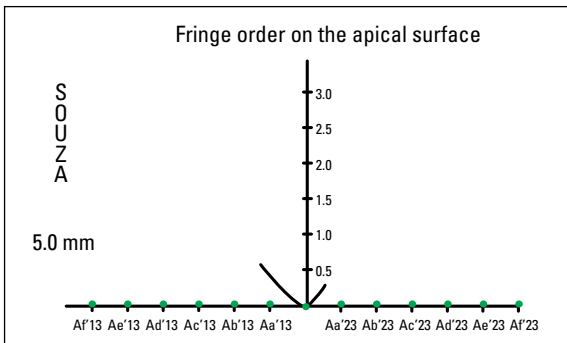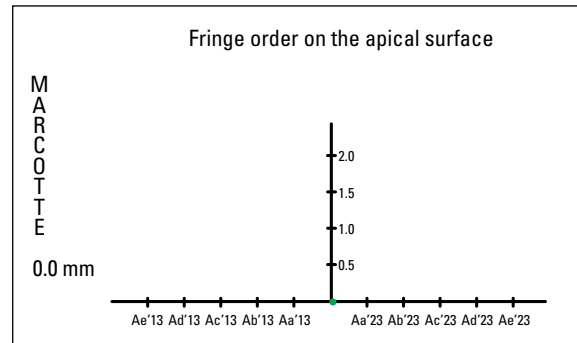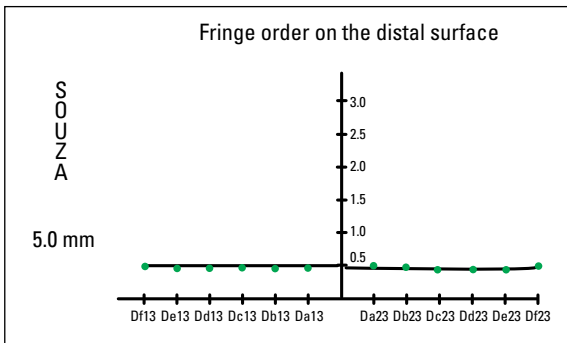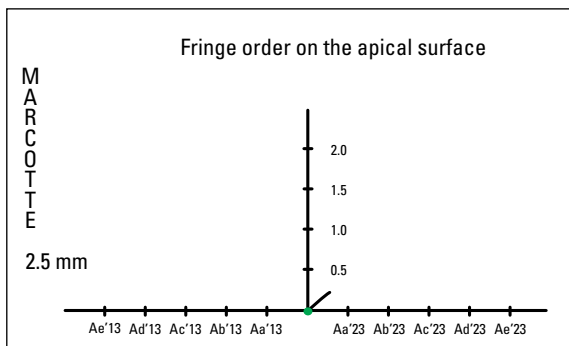

FIGURE 33 - Representation of the apical surface with Marcotte's preactivation and 2.5 mm activation
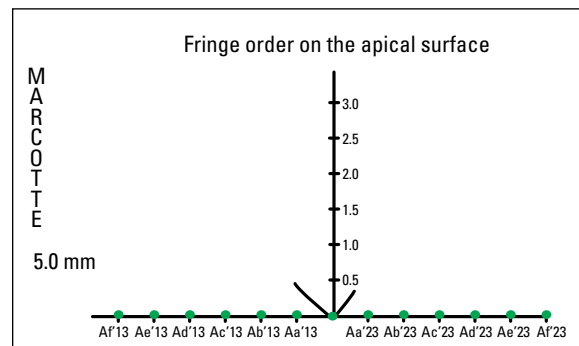
FIGURE 36 - Representation of the apical surface with Marcotte's preactivation and 5.0 mm activation.
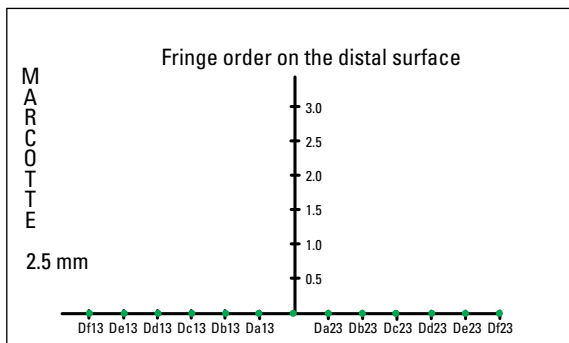
FIGURE 34 - Representation of the distal surface with Marcotte's preactivation and 2.5 mm activation.
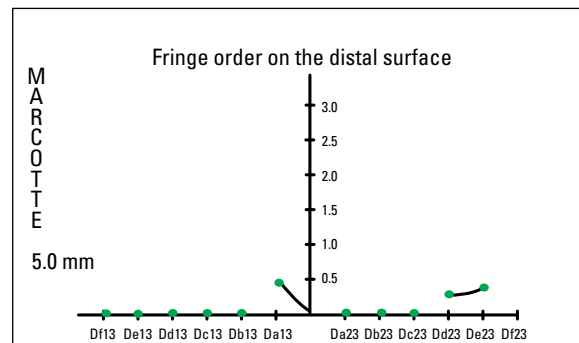
FIGURE 37 - Representation of the distal surface with Marcotte's preactivation and 5.0 mm activation.

DISCUSSION

Space closure in orthodontics should be performed as required in each particular case.[2,3,4,6,11,13,14,17-24] An appropriate choice of mechanism requires in-depth knowledge of the biomechanics built into the different retraction devices as well as the force systems they deliver. To this end, space closing springs should deliver a low load/deflection rate and a high momentum/force ratio, thereby enabling adequate tooth movement control.

The purpose of this study was to evaluate, us-

ing the experimental photoelastic method, the centered T-spring force system with two types of preactivation, 30 degrees[20] and 45 degrees.[14,21]

The photoelastic phenomenon was introduced in 1935 by an orthodontist[25] who used sculpted resin teeth with photoelastic properties to assess the areas of pressure and tension in their roots under force application. Since then, photoelasticity has played a prominent role in any research aimed at evaluating the properties of dental materials that undergo some form of intraoral force.[6,8,9,15] It is based on the fact that transparent materials become optically active under load situations when illuminated by monochromatic light. Thus, light and dark lines intersperse to form what is known as isochromatic and isoclinal lines. This optical effect is called photoelastic fringe and it reflects the stress or deformation experienced by a body, being measured both qualitatively and quantitatively.[9]

This method assesses the state of initial tension during the initial tooth movement phase[13] as recorded by a device named polariscope, which uses the properties of polarized light in its operation. These waves are used to determine the tension state through the light interference pattern,[7] comprised of a lighting system, a pair of polarizers and a structure to sustain and stabilize the model being analyzed.[8]

To determine the qualitative results of the order of isochromatic and isoclinal fringes a large number of points and measures is required, as well as time to obtain and interpret the fringes. After taking photographs, the images should be printed, parameters should be plotted and a fringe order map built to obtain the results.

Initially, tests were performed on pilot models in order to determine proper methodology research, materials to be used, number of repetitions needed, model fabrication technique, reading technique and researcher calibration to ensure result accuracy.[15]

For the construction of an ideal photoelastic model some basic principles were followed to avoid errors. The use of multirooted teeth in photoelastic models can compromise result interpretation due to overlapping fringes, which may occur as a result of root proximity.[4,6]

The use of resinous materials with slow return under stress conditions, providing residual stress before and after the withdrawal of forces were avoided. It should also, necessarily, have a low elasticity modulus, high strength and optical constant, while being easy to handle and be affordable.[15]

When the interest in studying the T-spring in photoelastic models aroused, considering that the study would be limited to initial tooth movements only, it was defined that only the initial activation pattern (neutral) would be analyzed, and eventually the spring's intermediate activation and finally its maximum activation would be evaluated. According to Burstone and Koenig,[2,3] the maximum T-spring activation would be 6.0 mm and the neutral position, 0.0 mm. Other authors believe that maximum activation would be 5.0 mm and in a neutral position T-springs would exhibit an activation of 2.0 mm.[14,20,21]

Titanium-molybdenum was the preferred alloy to fabricate T-springs, since it would be the most suitable, from a clinical standpoint, given its lower force magnitude[24] compared with stainless steel wire.[19,22,23]

When a T-spring is centered in the interbracket space it displays similar values for the forces system delivered by the segments of the anchorage and retraction units[10,17,20,21], which result from the symmetrical V-shaped preactivation bend. Clinically, the outcome is a more symmetrical tooth movement.

In analyzing the charts, it was noted that, in neutral position, both the 30° and the 45° preactivations on the apical base caused the distribution of photoelastic fringes to occur symmetrically. A difference was found in the number of fringes, which increased gradually with increasing activation and consequently generated a greater

force magnitude. By comparing force magnitude between the two preactivations (Figs 23 and 35), it is clear that the greatest magnitude occurred in the 30° preactivation.

The position of the T-spring in the inter-bracket space and the amount of activation are directly linked to the type of movement produced by the spring. When the T-spring is activated at 5.0 mm, the M/F ratio is 7.6, which provides a controlled tipping movement because its center of rotation is positioned more apically.[3] After 1.0 mm of deactivation, the M/F ratio is 9.1, which causes teeth to move by translation. Should this deactivation persist, tooth movement will occur by root movement[3] and at this time the spring should be reactivated to avoid contact between the roots of teeth adjacent to dental extractions.

In this experimental study, which used photoelastic models, we observed a higher concentration of photoelastic fringes in the cervical mesial region and no fringes on the distal apical region, at maximum activation of both springs. As deactivation occurred, this fringe order decreased in the cervical mesial region and increased in the mesial apical region until the fringe order reached higher energy concentration in the mesial apical region and lower concentration in the cervical mesial and distal apical regions. In light of these qualitative features, we can deduce that at maximum activation the springs exhibited a tendency toward root movement at 0.0 mm activation, bodily movement at medium activation and ultimately, at maximum activation,

controlled tipping movement.

An analysis of Figures 14, 21, 22, 33, 36 and 37 showed that fringe orders lower than 0.5 were formed. Some asymmetry, observed in Figures 14, 20, 21, 22, 24, 33, 36 and 37, showed no significant values. Importantly, these asymmetries may be due to an eccentricity in the position of the T-spring or an asymmetry in its final design.

It is also noteworthy that the force system delivered in all test groups was symmetrical for both teeth (13 and 23). The results are consistent with those observed in mechanical tests,[3,11,19,20,21,23,24] which were strikingly similar.

CONCLUSIONS

After implementing the experimental photoelastic method for qualitative analysis of the force system delivered by centered T-springs made with 0.017 X 0.025-in TMA wire, we concluded that:

1. The tension state in all root surface for the T-spring with preactivation according to Souza et al[20] was slightly greater when compared to the T-spring with preactivation according to Marcotte[14].

2. With 2.5 mm or 5.0 mm activation, the fringe order exhibited a tendency toward controlled tipping movement.

3. The fringe order was not much different at 2.5 mm activation with 30° and 45° preactivations.

4. At 5.0 mm activation, the concentration of energy or force was clearly higher in both preactivations.

REFERENCES

1. Articolo LC, Kusy K, Saunders CR, Kusy RP. Influence of ceramic and stainless steel brackets on the notching of archwires during clinical treatment. Eur J Orthod. 2000 Aug;22(4):409-25.
2. Burstone CJ. The segmented arch approach to space closure. Am J Orthod. 1982 Nov;82(5):361-78.
3. Burstone CJ, Koenig HA. Optimizing anterior and canine retraction. Am J Orthod. 1976 Jul;70(1):1-19.
4. Burstone CJ, Pryputniewicz RJ. Holographic determination of centers of rotation produced by orthodontic forces. Am J Orthod. 1980 Apr;77(4):396-409.
5. Chaconas SJ, Caputo AA, Davis JC. The effects of orthopedic forces on the craniofacial complex utilizing cervical and headgear appliance. Am J Orthod. 1976 May;69(5):527-39.
6. Chaconas SJ, Caputo AA, Miyashita K. Force distribution comparisons of various retraction archwires. Angle Orthod. 1989 May;59(1):25-30.
7. Dally JW, Rilley WF. Experimental stress analysis. New York: McGrall-Hill; 1965.
8. Glickman I, Roeber FW, Brion M, Pameijer JHN. Photoelastic analysis of internal stresses in the periodontium created by occlusal forces. J Periodontol. 1970 Jan;41(1):30-5.
9. Haraldson T. Photoelastic study of some biomechanical factors affecting the anchorage of osseointegrated implants in the jaw. Scand J Plast Reconstr Surg. 1980;14(3):209-14.
10. Hoenigl KD, Freudenthaler J, Marcotte MR, Bantleon HP. The centered T-loop: a new way of preactivation. Am J Orthod Dentofacial Orthop. 1995 Aug;108(2):149-53.
11. Kuhlberg AJ, Burstone CJ. T-loop position and anchorage control. Am J Orthod Dentofacial Orthop. 1997 Jul;112(1):12-8.
12. Kusy RP, Whitley JQ. Friction between different wire-bracket configurations and materials. Semin Orthod. 1997;3(3):166-77.
13. Lotti RS, Mazzieiro ET, Landre J Jr. A influência do posicionamento da alça T segmentada durante o movimento de retração inicial. Uma avaliação pelo método dos elementos finitos. Rev Dental Press Ortod Ortop Facial. 2006 maio-jun;11(3):41-54.
14. Marcotte MR. Biomecânica em Ortodontia. São Paulo: Ed. Santos; 1993.
15. Oliveira EJ. Material e técnica para análise fotoelástica plana da distribuição de tensões produzidas por implantes odontológicos. [dissertação]. Uberlândia (MG). Universidade Federal de Uberlândia; 2003.
16. Reitan K. Continuous bodily tooth movement and its histological significance. Acta Odontol Scand. 1947;7:115-44.
17. Shimizu RH. Fechamento de espaços após exodontias de primeiros pré-molares. [dissertação]. Araraquara (SP). Universidade Estadual Paulista; 1995.
18. Shimizu RH. Estudo dos sistemas de forças gerados pelas alças ortodônticas para fechamento de espaços. [tese]. Araraquara (SP). Universidade Estadual Paulista; 1999.
19. Shimisu RH, Sakima T, Santos-Pinto A, Shimizu IA. Desempenho biomecânico da alça "T", construída com fio de aço inoxidável, durante o fechamento de espaços no tratamento ortodôntico. Rev Dental Press Ortod Ortop Facial. 2002 nov-dez;7(6):49-61.
20. Souza RS, Santos-Pinto A, Shimizu RI, Sakima MT, Gandini LG Jr. Avaliação do sistema de forças gerado pela alça T de retração, pré-ativada segundo o padrão UNESP-Araraquara. Rev Dental Press Ortod Ortop Facial. 2003 set-out;8(5):113-22.
21. Souza RS, Shimizu RI, Sakima MT, Santos-Pinto A, GandinI LG Jr. Avaliação do sistema de forças gerado pela alça T de retração pré-ativada segundo o padrão Marcotte. JBO: J Bras Ortod Ortop Facial. 2005;10(55):50-8.
22. Thiesen G, Rego MVNN, Menezes LM, Shimizu RH. Avaliação biomecânica de diferentes alças ortodônticas de fechamento de espaços confeccionadas com aço inoxidável. Rev Assoc Paul Especial Ortod Ortop Facial. 2004 abr-jun;2(2):77-92.
23. THiesen G, Rego MVN, Menezes LM. A pré-ativação de alças ortodônticas para fechamento de espaços e seu efeito no sistema de forças gerado. Ortodontia Gaúcha. 2004 jan-jun;8(1):42-59.
24. Thiesen G, Rego MVNN, Menezes LM, Shimizu RH. A utilização de diferentes configurações de molas T para obtenção de sistemas de forças otimizados. Rev Dental Press Ortod Ortop Facial. 2006 set-out;11(5):57-77.
25. Zak B. Photoelastiche analyse in der orthodontischen mechanik. Z Stomatol. 1935;33:22-37.

Contact address
Luiz Guilherme Martins Maia
Rua Terêncio Sampaio, 309
CEP: 49.025-700 – Aracaju / SE, Brazil
E-mail: orthomaia2003@yahoo.com.br